NATIONAL ADVISORY COMMITTEE FOR AERONAUTICS

TECHNICAL NOTE 3463

INVESTIGATION OF THE VIBRATIONS OF A HOLLOW THIN-WALLED RECTANGULAR BEAM

By Eldon E. Kordes and Edwin T. Kruszewski

Langley Aeronautical Laboratory
Langley Field, Va.

Washington
October 1955

NATIONAL ADVISORY COMMITTEE FOR AERONAUTICS

TECHNICAL NOTE 3463

INVESTIGATION OF THE VIBRATIONS OF A HOLLOW THIN-WALLED RECTANGULAR BEAM

By Eldon E. Kordes and Edwin T. Kruszewski

SUMMARY

Experimental modes and frequencies of an unstiffened hollow beam of rectangular cross section are presented, and comparisons are made between experimental and theoretical frequencies. Theories based on rigid cross sections were found to be sufficiently accurate to predict the frequencies of only the lowest three bending modes. For the higher bending modes and all the torsional modes it was necessary to include the effects of cross-sectional distortions in the calculations.

INTRODUCTION

The vibration characteristics of hollow thin-walled cylindrical beams have been investigated theoretically in references 1 and 2 for both bending and torsional vibrations. In reference 1, frequency equations that include the influence of transverse shear deformation, shear lag, and longitudinal inertia are derived for the bending vibrations of cylindrical beams with constant wall thickness. In reference 2, frequency equations that include the influence of warping restraint and longitudinal inertia are derived for the torsional vibrations.

In order to provide an experimental check on the theories of references 1 and 2, vibration tests were conducted on a hollow beam of rectangular cross section with no bulkheads. The purpose of the present paper is to present these experimental results and to show the accuracies that can be obtained from the theories of references 1 and 2 when the effects of cross-sectional deformation are taken into account by the methods presented in references 3 and 4.

EXPERIMENTAL INVESTIGATION

Description of Specimen

The specimen used in the experimental investigation (see fig. 1) was constructed from four aluminum sheets of equal thickness welded together along their lengths to form a uniform rectangular tube and contained no stringers, web stiffeners, or bulkheads. The beam, whose dimensions are shown in figure 1, had a width-depth ratio of 3.6 and a plan-form aspect ratio (length divided by width) of 13.3. The material from which the specimen was constructed, 3003 aluminum (formerly designated 3S), had a modulus of elasticity of 10.1×10^6 pounds per square inch, a shear modulus of 3.81×10^6 pounds per square inch, and a density of 0.098 pound per cubic inch.

Test Setup and Instrumentation

The general test setup is shown in figure 2. The test beam was supported at each end by means of long flexible wires attached to the center line of the top spar web. This type of support offered only negligible resistance to small displacements of the beam in the horizontal direction. For small amplitudes of vibration in the horizontal direction, therefore, the specimen was considered to be essentially free-free. A fitting for connecting the shaker to the beam was attached to one cover of the beam at a point slightly off center in both the chordwise and spanwise directions so that symmetrical and antisymmetrical bending and torsional modes could be excited without relocating the shaker attachment point.

An electromagnetic shaker mounted on a rigid backstop was used to vibrate the beam in the horizontal direction. The frequency of the exciting force was controlled by a continuously variable frequency audio oscillator which was connected to the shaker drive coil through a 500-watt power amplifier. The direct-current power for the shaker field was supplied by a motor-generator unit. The shaker system was capable of developing a maximum undistorted force output of 26 pounds from 20 to 1,600 cycles per second and a maximum double amplitude of 1/4 inch.

In order to obtain more accurate readings of the frequency values than were possible from the oscillator scale, a Stroboconn frequency meter was used to measure the frequency of the oscillator signal. In this frequency meter the oscillator output flashes a stroboscopic light onto a series of graduated disks revolving at controlled speeds. The disk speed and hence the frequency of vibration are known to be accurate within 0.01 percent.

A crystal phonograph pickup was used to study the motion of the vibrating beam. The pickup has a voltage output that is proportional to the velocity of motion and is essentially linear from 50 to 4,000 cycles per second. A cathode-ray oscilloscope was used to indicate the output of the pickup.

Experimental Test Procedure

The test beam and the electromagnetic shaker were mounted as shown in figure 2. The pickup was placed on a stand so that the probe just touched the beam. As a preliminary study of the vibration characteristics of this test beam, the force-amplitude controls of the shaker system were set at a constant value and the frequency was slowly increased from 20 to 650 cycles per second. During this study, each resonant frequency where the amplitude of vibration (as viewed on the oscilloscope) passed through a maximum was noted. As an aid in obtaining these various resonant frequencies, the phase angle between the applied force and the velocity of the beam was observed. This phase angle was determined by viewing the Lissajous ellipse shown on the oscilloscope when the pickup output was applied to one axis and the oscillator output to the other.

After the preliminary study was completed, each of the observed resonant frequencies was reestablished and held constant while a survey of the corresponding mode shape was made. This was done by moving the pickup along the beams and noting the location of the null points and the phase of the motion between the null points. The type of vibration and the relative amplitude of the various points on the test beam were thus established. In this manner, all beam bending and torsional modes in the frequency range from 20 to 650 cycles per second were identified. Once the mode of vibration was identified, the frequency was read from the frequency meter. As might be expected, resonances not associated with beam bending and torsional modes were observed during the test. These resonances were presumably due to local effects and are not considered in this report.

Experimental Results

In the frequency range covered by the tests, the first ten natural beam frequencies (five bending and five torsional) were obtained, and these frequency values and the nodal patterns corresponding to each of the natural frequencies f are shown in figures 3 and 4. These patterns for all but the fifth torsional mode are shown only for the front cover since they were essentially the same in both cover sheets. In the fifth torsional mode the nodal patterns in the two covers were different; both patterns are shown in figure 4. The nodal patterns for all the symmetrical modes (both bending and torsional) and for the lowest antisymmetrical

bending and torsional modes are definitely beam nodal patterns. For the remaining antisymmetrical modes, however, the nearness of the shaker attachment to the center line of the beam evidently caused a shifting of the nodal patterns. The tendency of the nodal lines to shift is probably increased by the absence of internal stiffening members in the test beam.

Amplitude surveys made to establish the nodal shapes disclosed an interesting phenomenon pertaining to the distortions of the cross section. For the higher bending modes, the deflections at the center line of the cover were from $1\frac{1}{2}$ to 3 times as great as the deflections of the corners of the tube. No such large distortions of the covers were evident for the torsional modes.

THEORETICAL CALCULATIONS AND COMPARISONS WITH EXPERIMENTAL RESULTS

Bending

A solution for the transverse vibrations of hollow thin-walled beams was presented in reference 1. The first five natural bending frequencies of the test beam were calculated from the frequency equations derived in reference 1 and are presented in table I along with the experimental frequencies and the frequencies calculated from elementary beam theory. The frequency equation and the values of the parameters used for these calculations are shown in appendix A.

Comparison of the results presented in table I shows that for all modes the frequencies calculated from the equations of reference 1 are in better agreement with experimental frequencies than with those calculated from elementary beam theory. For the first three modes, the agreement between the experimental frequencies and those calculated from reference 1 is within 12 percent. For the higher modes, however, the agreement is not very satisfactory.

Examination of the assumptions used in the derivation of the frequency equations in reference 1 shows that, although the influence of transverse shear, shear lag, and longitudinal inertia are included, the results are applicable only to cylindrical beams whose cross sections remain relatively undistorted. The particular test beam used in the experimental investigation contained no bulkheads, stiffeners, or stringers to help prevent cross-sectional distortions. Furthermore, as mentioned in the preceding section, results of the amplitude surveys showed that, for the higher modes of bending vibration, the covers of the beam vibrated out of their plane with considerable amplitude. The fact that these local cover or panel

vibrations can have appreciable effect on the beam vibrations is substantiated in reference 3 where it is shown that inertial coupling exists between the local panel vibrations and overall transverse vibrations. The result of this coupling is a reduction of the bending frequencies calculated for rigid cross sections. As is found in reference 3, this reduction is dependent on the uncoupled panel frequency (frequency of panel vibration with the overall beam vibration restrained). Methods are included therein for determining this uncoupled panel frequency and for estimating the reduction in bending frequencies due to panel vibrations.

The method of reference 3 has been used in appendix A to correct the calculated beam bending frequencies of the test beam for the effects of panel distortions. These corrected frequency values are shown in table I. From the results in this table it is seen that the effects of panel distortion are negligible for the first mode but become important for the higher modes. Also, the corrected frequencies are seen to compare very well with the experimental frequencies.

Torsion

A solution for the torsional vibrations of a hollow thin-walled beam was presented in reference 2. From the frequency equations derived in this reference the first five torsional frequencies of the test beam were calculated as shown in appendix A. These calculated frequencies are presented in table II along with the experimental frequencies. For completeness the frequencies calculated from elementary torsion theory are also included in table II.

Although the frequency equations of reference 2 include the effect of warping restraint and longitudinal inertia, examination of columns (2) and (4) in table II shows that the results from these equations do not predict the natural torsional frequencies with any degree of accuracy. The calculated frequency for the first torsional mode differs from that found experimentally by more than 25 percent, whereas the calculated frequency for the fifth mode is almost three times as large as the measured frequency.

Since the analysis used in reference 2 is based on the assumption that the distortions of the cross sections are negligible, the large discrepancies between calculated and experimental torsional frequencies could be due to cross-section distortions.

Reference 3 showed that panel flexibilities can have an effect on torsional frequencies similar to the coupling effect described for bending vibrations. For the particular test beam, however, the effects were found to be small - only a 3-percent reduction of the fifth torsional frequency. The reason for this small reduction is that, in the particular type of

panel vibration considered in reference 3, the corners of the beam do not move with respect to each other; no shearing distortions of the cross section are allowed. Since a beam in torsional oscillation is subjected to cross-sectional shearing forces, cross-sectional shear deformations should be considered.

The influence of shear flexibility of cross sections on the torsional frequencies of box beams was investigated in reference 4. As could be expected, one of the quantities on which this influence is dependent is the effective cross-sectional shear modulus of the beam cross section G_e. The test beam contains no internal bulkheads; therefore, the shear stiffness of the cross section is due only to the Vierendeel truss action of the rectangular bent formed by the walls of the tube. On the basis of the assumption of rigid joints at the corners, the effective shear modulus of a bent is determined in appendix B. From these results the value of G_e of 2,540 pounds per square inch for the test beam is calculated in appendix A.

On the basis of this value of G_e, the torsional frequencies of the test beam have been recalculated in appendix A by the method of reference 4.

Examination of these results shows that, with the inclusion of shear flexibility of the cross section, there is a considerable reduction in the calculated frequencies. The percentage reduction, however, is still short of that necessary for good agreement between calculated and experimental frequencies. Since the tube consisted of aluminum sheets welded along the corners, a poor or incompletely penetrating weld would result in flexible corner joints and, consequently, in a reduction in the value of G_e from that calculated by use of the equation derived in appendix B. In order to check the completeness of the weld, sections were cut from corners of the test beam and were prepared for microscopic study. A photomicrograph of a typical section of the weld is shown in figure 5 and it can be seen that, although the weld itself is sound, the depth of penetration is less than half the depth of the material. Thus, the assumption of rigid corners used in the calculation of G_e would not be expected to apply to the test beam, and the calculated value of G_e would be too large.

In order to obtain a value for the effective shear modulus of the cross section that is appropriate for the test beam, a value of G_e was determined experimentally. Several 1-inch slices were cut from the test beam and loaded diagonally, and the change in length of the diagonals was measured. From the results of these tests, the measured values of G_e were found to range from 1,080 to 1,520 pounds per square inch with an average value of 1,290 pounds per square inch. This average value of G_e was then used and the calculation based on the analysis of reference 4 was repeated.

Results of calculations for this measured value of G_e are shown in table II. It is seen that good agreement exists between these frequencies and the experimental frequencies. These results indicate that, once the effective shear modulus of the cross section is known, the results of reference 4 can predict natural torsional frequencies with good accuracy.

It should be pointed out that the final results based on reference 4 do not include the effect of longitudinal inertia. The effects, however, were shown in reference 2 to be negligible for the values of plan-form aspect ratio of the test beam.

CONCLUSIONS

The first ten natural beam modes and frequencies obtained from vibration tests of a hollow beam of rectangular cross section are presented. From comparisons made between these experimental and calculated frequencies, the following conclusions can be made:

1. The frequency equation derived in NACA Rep. 1129 predicts the frequencies of transverse vibration of tubes with reasonable accuracy as long as the effect of panel vibrations is small.

2. Local panel vibrations can have an appreciable influence on the higher transverse modes of vibrations of tubes. The analysis of NACA TN 3070, however, predicts the correction for the effect of local panel flexibilities very well.

3. For beams, such as the test beam, which have very flexible cross sections, the torsional frequency equations derived in NACA TN 3206 are not directly applicable.

4. The effect of local panel vibrations on the torsional frequencies of the test beam was small. The effect of shear distortion of the cross section, however, was large because of the absence of bulkheads, but the effect of this distortion on torsional frequencies is predicted very satisfactorily by the theory derived in NACA TN 3464.

Langley Aeronautical Laboratory,
National Advisory Committee for Aeronautics,
Langley Field, Va., April 13, 1955.

APPENDIX A

CALCULATION FOR BEAM VIBRATION MODES

Beam Bending Modes

The frequency equations for symmetrical and antisymmetrical free-free beam bending modes are given by equations (41) and (52), respectively, in reference 1 and are repeated here for convenience.

For the symmetrical modes

$$k_B^2\left[1 + k_B^2 \sum_{n=1,3,5}^{\infty}\left(\frac{2}{n\pi}\right)^2\frac{1}{N_n}\right] = 0 \tag{A1}$$

and for the antisymmetrical modes

$$k_B^2\left[\sum_{n=2,4,6}^{\infty}\left(\frac{2}{n\pi}\right)^2\frac{k_B^2}{N_n} + \frac{2}{\pi^2}\frac{A}{A_S}k_{RI}^2\sum_{n=1,2,3}^{\infty}\frac{A_n^2}{B_0^2k_S^2 + K^2n^2} + \frac{1}{3}\right] = 0 \tag{A2}$$

where, for cylindrical beams of rectangular cross section,

$$N_i = \frac{i^2\pi}{8k_S^2}\left\{\pi - \frac{K}{4k_SB_i}\frac{p}{a}\left[\frac{\sinh\frac{\pi}{2}\frac{k_S}{K}B_i\left(\frac{8a}{p} - 1\right)}{\cosh\frac{\pi}{2}\frac{k_S}{K}B_i} + \tanh\frac{\pi}{2}\frac{k_S}{K}B_i\right]\right\} - \frac{1}{2}k_B^2 = 0 \tag{A3}$$

In these equations k_B is the frequency parameter defined as $k_B^2 = \frac{\mu L^4}{EI_y}\omega_B^2$ where ω_B is the natural circular frequency in radians per second.

In this section and in those that follow, the equations presented and the symbols used are the same as in the reference for the particular section. Therefore, the reader is cautioned to observe that the definitions for symbols are not interchangeable. For this reason, most of

the symbols are defined separately in each section. The following symbols, however, are the same throughout:

a	half-depth of beam measured from median line, 1.00 in.
b	half-width of beam measured from median line, 3.60 in.
s	distance along perimeter of cross section
t	wall thickness, 0.246 in.
L	half-length of beam, 47.86 in.
p	perimeter of cross section, 18.40 in.
E	modulus of elasticity, 10.1×10^6 lb/in.^{2}
G	shear modulus of elasticity, 3.81×10^6 lb/in.^{2}
i,n	integers

The various parameters given in reference 1 are defined and their numerical values for test beams are given as follows:

μ	mass of beam per unit length, 1.15×10^{-3} lb-sec^2/in.^{2}
A	cross-sectional area, 4.52 in.^{2}
I_y	minimum moment of inertia of cross section, 3.87 in.^{4}
k_B	frequency coefficient, $1.24\omega_B \times 10^{-2}$
k_S	coefficient of shear rigidity, $\sqrt{\frac{EI_y}{L^2 A_S G}} = 6.74 \times 10^{-2}$
k_{RI}	coefficient of rotary inertia, $\sqrt{\frac{I_y}{AL^2}} = 1.932 \times 10^{-2}$
K	geometrical parameter, $\sqrt{\frac{16 I_y}{A_S p^2}} = 0.431$
B_i	parameter, $\sqrt{i^2 - k_{RI}^2 \left(\frac{2}{\pi}\right)^2 k_B^2} = \left(i^2 - 1.513 k_B^2 \times 10^{-4}\right)^{1/2}$
A_S	effective shear-carrying area, $\oint t \sin^2\theta \, dS = 0.984$ in.^{2}

A_n Fourier coefficient,

$$\frac{2}{p}\oint \sin\theta \sin\frac{2n\pi s}{p}\,ds = 0 \qquad \text{(n even)}$$

$$= \frac{1.273}{n}\cos 1.23n \qquad \text{(n odd)}$$

θ inclination of normal with vertical

The numerical values given for the aforementioned various parameters were used, and the natural frequencies of bending vibration were calculated from equations (A1) and (A2) by trial.

Local Panel Vibration

The procedure recommended in reference 3 for estimating the effect of local panel vibrations on the vibrations of box beams was used to correct the calculated beam bending frequencies of the test beam. These corrections were made as follows:

(1) The values of the "uncoupled" bending frequencies were taken as the values given in column (3) of table I.

(2) By using the width-depth ratio of 3.6 and the thickness ratio of 1, the values of the uncoupled member frequency of 833 cycles per second and the coupling constant of 0.58 were obtained from figures 7 and 8 of reference 3.

(3) The values of the coupled frequencies corresponding to the values of uncoupled frequency shown in column (3) of table I were then determined from figure 6 of reference 3.

Beam Torsion Modes

The frequency equations for the free-free beam torsion modes (eqs. (40) and (51) of ref. 2) for the symmetrical modes are

$$k_T^2\left[1 + k_T^2 \sum_{n=1,3,5}^{\infty}\left(\frac{2}{n\pi}\right)^2 \frac{1}{N_n}\right] = 0 \qquad \text{(A4)}$$

and for the antisymmetrical modes are

$$k_T^2\left[\frac{pt_a\mu}{2I_p}\left(\frac{2p}{\pi L}\right)^2 \sum_{n=2,4,6}^{\infty} \frac{K_n^2}{B_0^2 + 16n^2} + \left(\frac{2}{\pi}\right)^2 k_T^2 \sum_{n=2,4,6}^{\infty} \frac{1}{n^2 N_n} + \frac{1}{3}\right] = 1 \qquad (A5)$$

In equations (A4) and (A5), k_T is the torsional frequency parameter and is defined as $k_T^2 = \frac{I_p L^2}{GJ}\omega_T^2$ where ω_T is the natural circular frequency in radians per second.

For cylindrical beams of rectangular cross section,

$$N_i = \frac{(i\pi)^2}{8}\left\{1 + \left(\frac{a^2 - b^2}{ab}\right)^2\left[\frac{ab}{4(a+b)^2} + \frac{1}{\pi B_i}\left(\frac{\cosh\frac{\pi B_i}{8}\frac{a-b}{a+b}}{\sinh\frac{\pi B_i}{8}} - \coth\frac{\pi B_i}{8}\right)\right]\right\} - \frac{1}{2}k_T^2 \qquad (A6)$$

The various parameters appearing in equations (A4), (A5), and (A6) as defined in reference 2 are given as follows:

ρ distance from centroid of cross section to tangent to the median line of wall thickness

μ mass density of beam, 8.16×10^{-3} lb-sec^2/in.^{4}

A_0 cross-sectional area enclosed by median line of wall thickness, $4ab = 14.40$ in.^{2}

I_y minimum moment of inertia of cross section about y-axis, 3.87 in.^{4}

I_z maximum moment of inertia of cross section about z-axis, 27.96 in.^{4}

I_p mass polar moment of inertia per unit length, $\mu(I_y + I_z) = 8.08 \times 10^{-3}$ lb-sec^2

J torsional stiffness constant, $\frac{4A_0^2t}{p} = 11.06$ in.^{4}

$k_T = 6.63\omega_T \times 10^{-4}$

k_{LI} coefficient of longitudinal inertia, $\sqrt{\frac{Jp^2\mu}{I_pL^2}} = 0.227$

K parameter, $\sqrt{\frac{Ep^2}{GL^2}} = 0.626$

t_a actual wall thickness

B_i parameter, $\sqrt{K^2i^2 - k_{LI}^2\left(\frac{2}{\pi}\right)^2k_T^2} = \left(0.391i^2 - 0.0209k_T^2\right)^{1/2}$

$B_0 = B_i$ for $i = 0$

K_0 Fourier constant, $\frac{1}{p}\oint \rho \, ds = 1.565$ in.

K_n Fourier coefficient,

$$\frac{2}{p}\oint \rho \cos\frac{2n\pi s}{p} \, ds = -3.304 \sin 1.23n \quad \text{(n even)}$$

$$= 0 \quad \text{(n odd)}$$

The roots of the frequency equations (A4) and (A5) were obtained by trial.

Shear Deformation of the Cross Section

The analysis of the torsional vibration of box beams where the effect of shear distortion of the cross section is included is presented in reference 4. The appropriate frequency equation, based on a four-flange box beam, for symmetrical vibration is

$$1 + 2\sum_{n=1,2,3}^{\infty} \frac{\left(k_{b_0}^2 - \frac{k_T^2}{1-c^2}\right)(n\pi)^2 - k_T^2\left(k_{b_0}^2 - k_T^2\right)}{\frac{K^2}{1-c^2}(n\pi)^6 + K^2\left(k_{b_0}^2 - k_T^2M\right)(n\pi)^4 + \left[k_{b_0}^2 - \frac{k_T^2}{1-c^2} - \frac{K^2k_T^2}{B}\left(k_{b_0}^2 - k_T^2\right)\right](n\pi)^2 - k_T^2\left(k_{b_0}^2 - k_T^2\right)} = 0 \quad \text{(A7)}$$

and for antisymmetrical vibration is

$$\sum_{n=1,3,5}^{\infty} \frac{\left(k_{b_0}^2 - \frac{k_T^2}{1 - C^2}\right)\left(\frac{n\pi}{2}\right)^2 - k_T^2\left(k_{b_0} - k_T^2\right)}{\frac{K^2}{1 - C^2}\left(\frac{n\pi}{2}\right)^6 + K^2\left[k_{b_0}^2 - k_T^2 M\right]\left(\frac{n\pi}{2}\right)^4 + \left[k_{b_0}^2 - \frac{k_T^2}{1 - C^2} - \frac{K^2 k_T^2}{B}\left(k_{b_0}^2 - k_T^2\right)\right]\left(\frac{n\pi}{2}\right)^2 - k_T^2\left(k_{b_0}^2 - k_T^2\right)} = 0 \qquad (A8)$$

where

A parameter, $\frac{b^2 - a^2}{4ab} = 0.829$

A_F area of flange, $\frac{t}{3}(a + b) = 0.377$

B parameter, $\frac{(a + b)^2}{4ab} = 1.468$

C inertia coupling constant, $\frac{I_z - I_y}{I_z + I_y} = 0.757$

G_e effective shear modulus of bulkheads

K restraint-of-warping parameter, $\left(\frac{EA_F}{4GL^2}\frac{a + b}{t} = 2.04 \times 10^{-3}\right)^{1/2}$

k_T frequency coefficient, $\omega_T\sqrt{\frac{I_p L^2}{GJ}}$

k_{b_0} frequency coefficient for uniform shear mode, $\left(\frac{S}{1 - C^2} = 18.62\right)^{1/2}$

M parameter, $\frac{2}{1 - C^2}\left(1 - \frac{AC}{B}\right) = 2.68$

S bulkhead stiffness parameter, $\frac{G_e L^2}{Gab}\frac{a + b}{t} = 7.95$

ω_T natural torsional frequency of four-flange box beam

The effective shear modulus of the cross section is determined in appendix B of this paper for the test beam and is given by

$$G_e = \frac{3D}{ab(a + b)} = 2{,}540 \text{ lb/in.}^2 \tag{A9}$$

where

$$D = \frac{Et^3}{12\left(1 - \nu^2\right)}$$

and ν is Poisson's ratio.

APPENDIX B

EFFECTIVE SHEAR MODULUS OF CROSS SECTION

In this appendix the effective shear modulus of a rectangular bent is determined. For the analysis, the members of the bent are assumed to be plate elements and the corners are assumed to remain right angles. The deflections and bending moments due to an applied load P are as shown in the following sketch:

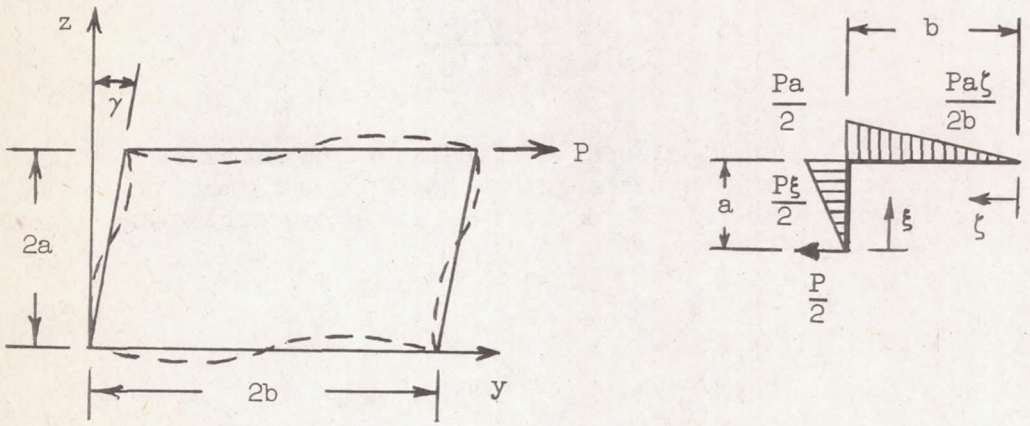

The strain energy for a bent of unit width is

$$U = \frac{2}{D}\int_0^a \left(\frac{P\xi}{2}\right)^2 d\xi + \frac{2}{D}\int_0^b \left(\frac{Pa\zeta}{2b}\right)^2 d\zeta = \frac{P^2a^2}{6D}(a + b) \qquad (B1)$$

where $D = \frac{Et^3}{12\left(1 - \nu^2\right)}$ and ξ and ζ are coordinates. In terms of the angle γ and the effective shear modulus of the section G_e, the strain energy for a unit width is

$$U = 2G_e\gamma^2ab \qquad (B2)$$

The relation between the angular displacement γ and the load P can be obtained from equation (B1) by the use of Castigliano's theorem,

and their relation is

$$\gamma = \frac{Pa^2}{6aD}(a + b) \tag{B3}$$

Substituting equation (B3) into equation (B2) and equating the energy expressions from equations (B1) and (B2) gives the following expression for the effective shear modulus of the rectangular bent:

$$G_e = \frac{3D}{ab(a + b)} \tag{B4}$$

For the test beam, the shear stiffness of the cross section is due to the truss action of the rectangular bent formed by the tube walls. Thus, the effective shear modulus of the beam cross section is given by equation (B4).

REFERENCES

1. Budiansky, Bernard, and Kruszewski, Edwin T.: Transverse Vibrations of Hollow Thin-Walled Cylindrical Beams. NACA Rep. 1129, 1953. (Supersedes NACA TN 2682.)

2. Kruszewski, Edwin T., and Kordes, Eldon E.: Torsional Vibrations of Hollow Thin-Walled Cylindrical Beams. NACA TN 3206, 1954.

3. Budiansky, Bernard, and Fralich, Robert W.: Effects of Panel Flexibility on Natural Vibration Frequencies of Box Beams. NACA TN 3070, 1954.

4. Kruszewski, Edwin T., and Davenport, William W.: Influence of Shear Deformation of the Cross Section on Torsional Frequencies of Box Beams. NACA TN 3464, 1955.

TABLE I

FREQUENCIES OF BENDING VIBRATIONS

Mode	Experimental frequency, cps	Calculated frequencies, cps			
		Undistorted cross-section theory		Coupled bending-panel theory (ref. 3)	Percent difference (based on experiment)
		Elementary bending	Reference 1		
①	②	③	④	⑤	⑥
1	68.7	71.5	70.2	70.2	2.2
2	184	197	187	183	-.7
3	342	385	348	328	-4.1
4	464	638	545	474	2.2
5	572	953	761	586	2.5

TABLE II

FREQUENCIES OF TORSIONAL VIBRATIONS

Mode	Experimental frequency, cps	Calculated frequencies, cps				
		Undistorted cross-section theory		Flexible cross-section theory (ref. 4)		Percent difference (based on experiment)
		Elementary torsion	Reference 2	Calculated G_e	Measured G_e	
①	②	③	④	⑤	⑥	⑦
1	301	376	377	343	316	5.0
2	404	751	753	539	435	7.7
3	455	1,128	1,133	627	485	6.6
4	530	1,501	1,515	706	561	5.8
5	648	1,880	1,911	825	705	8.9

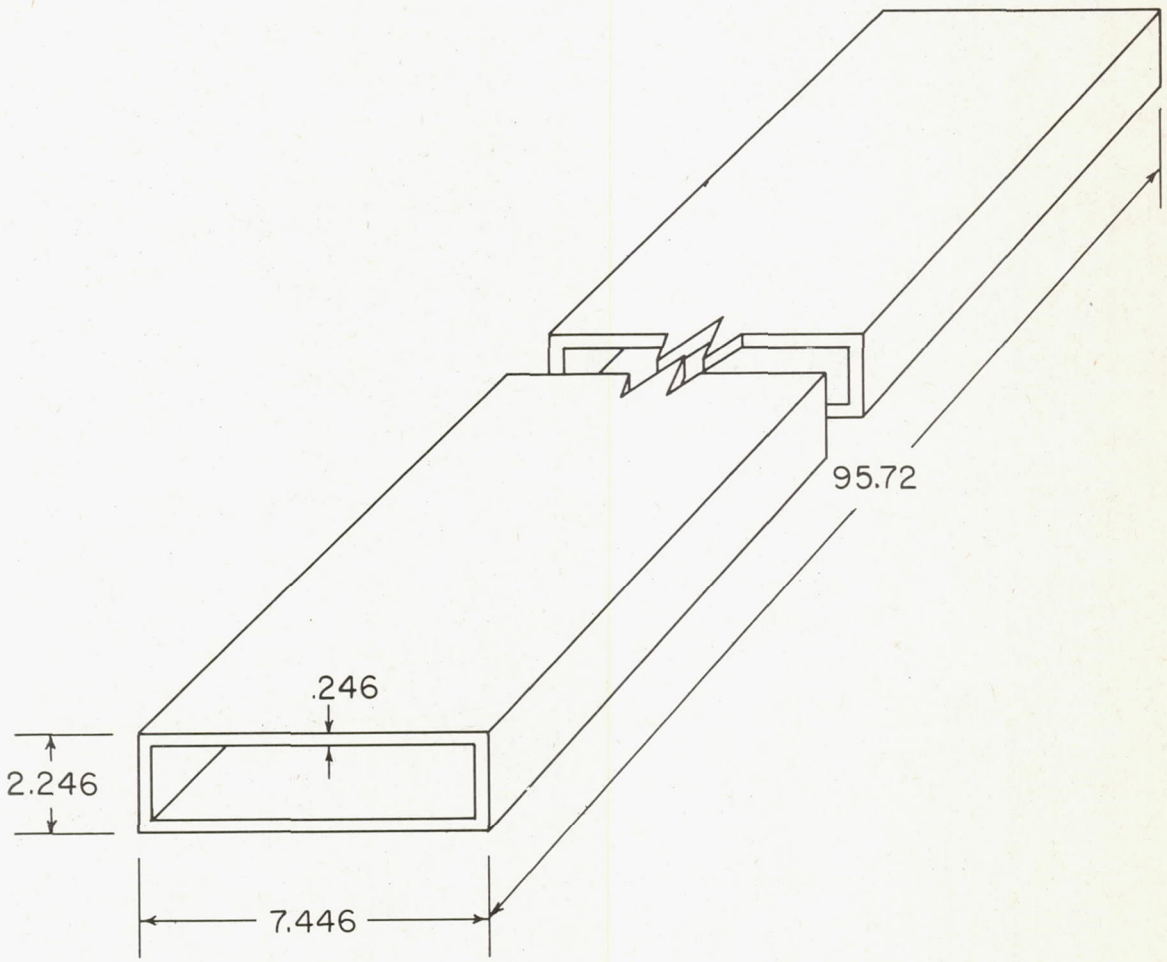

Figure 1.- Test specimen.

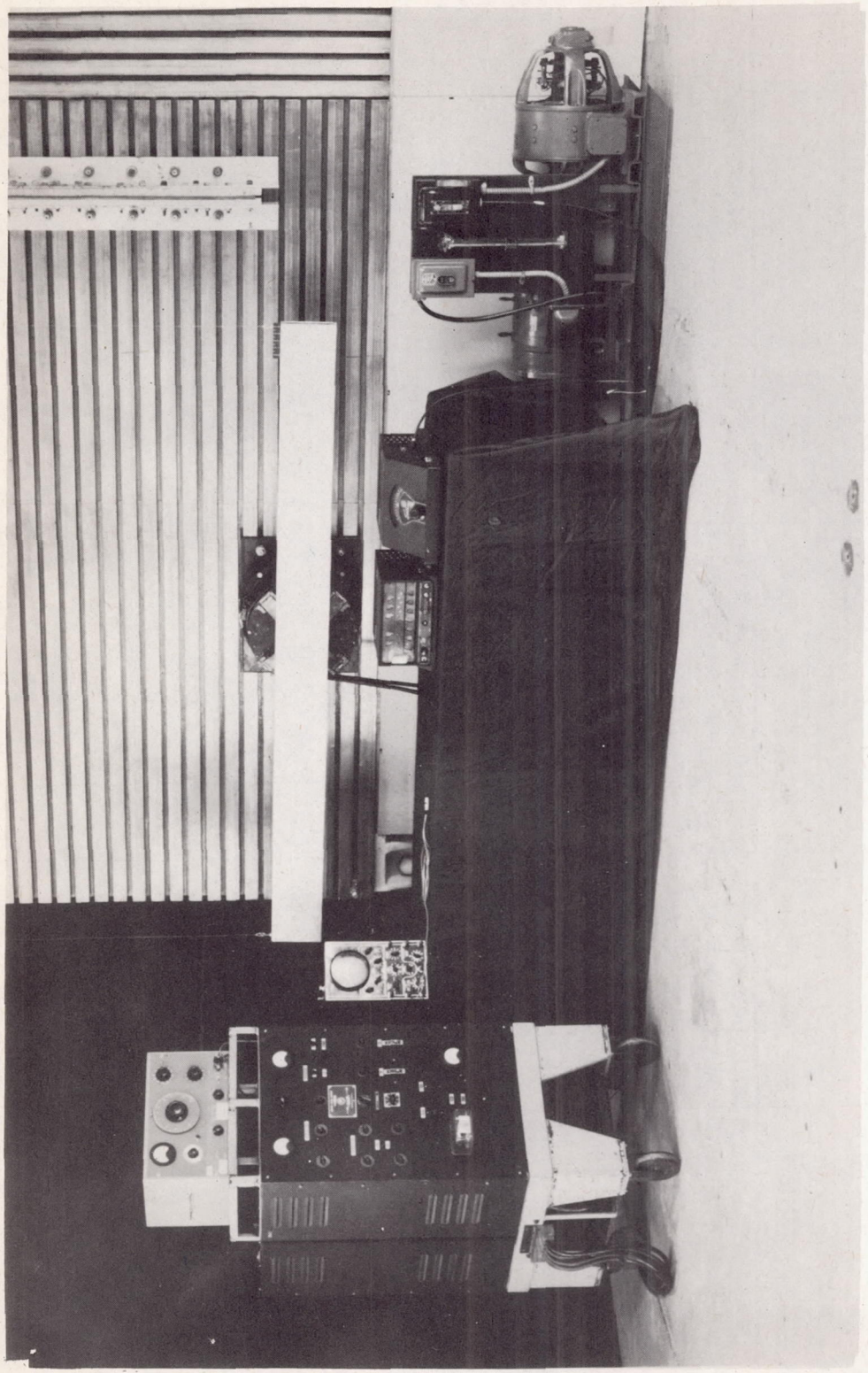

L-77728

Figure 2.- Test setup.

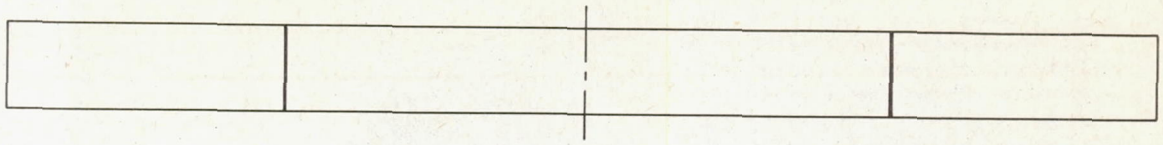

(a) First symmetrical mode.
f= 68.7 cps.

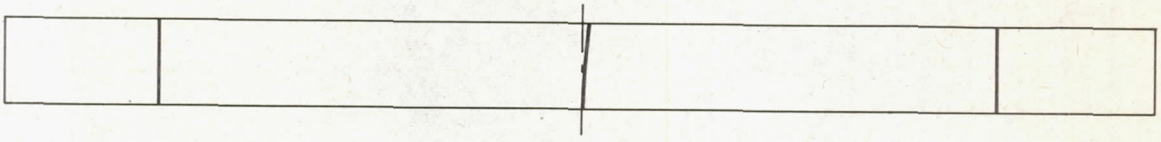

(b) First antisymmetrical mode.
f= 184 cps.

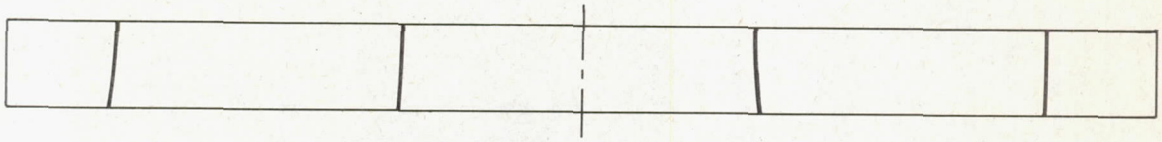

(c) Second symmetrical mode.
f= 342 cps.

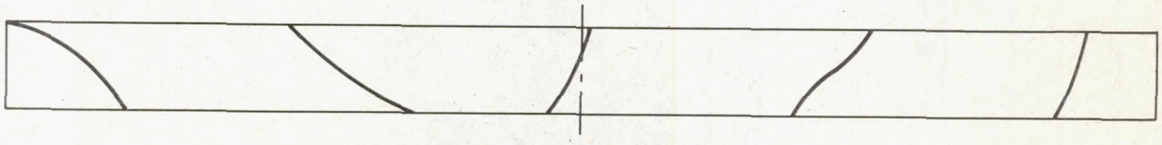

(d) Second antisymmetrical mode.
f= 464 cps.

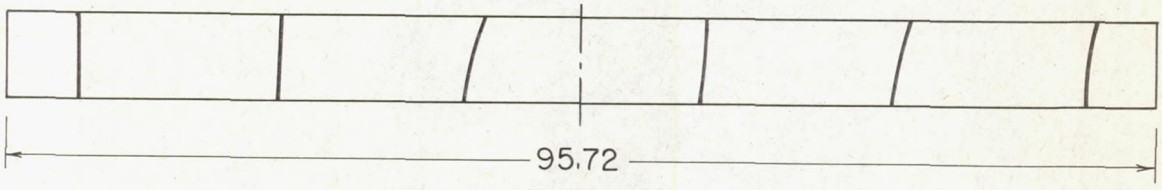

(e) Third symmetrical mode.
f= 572 cps.

Figure 3.- Nodal pattern for first five bending modes of test beam.

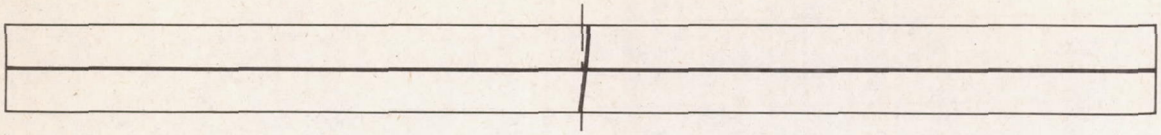

(a) First antisymmetrical mode.
f= 301 cps.

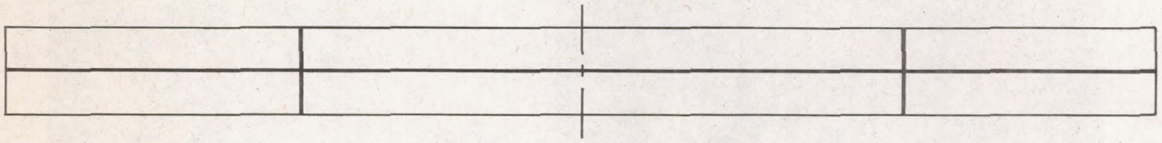

(b) First symmetrical mode.
f= 404 cps.

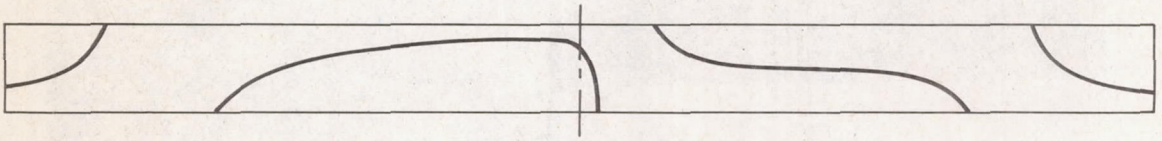

(c) Second antisymmetrical mode.
f= 455 cps.

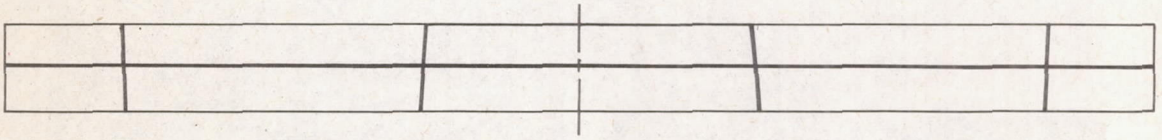

(d) Second symmetrical mode.
f= 530 cps.

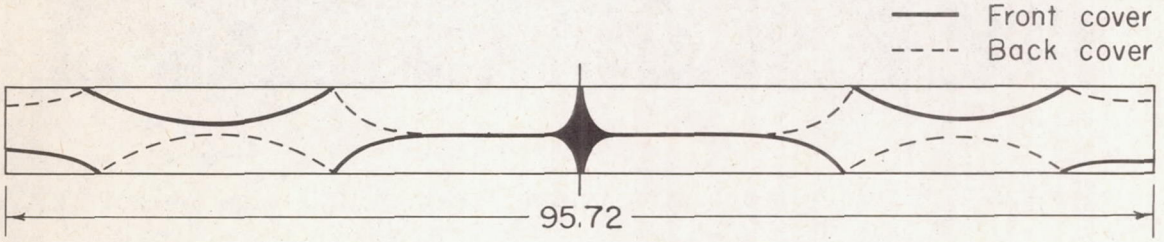

(e) Third antisymmetrical mode.
f= 648 cps.

Figure 4.- Nodal pattern for first five torsional modes of test beam.

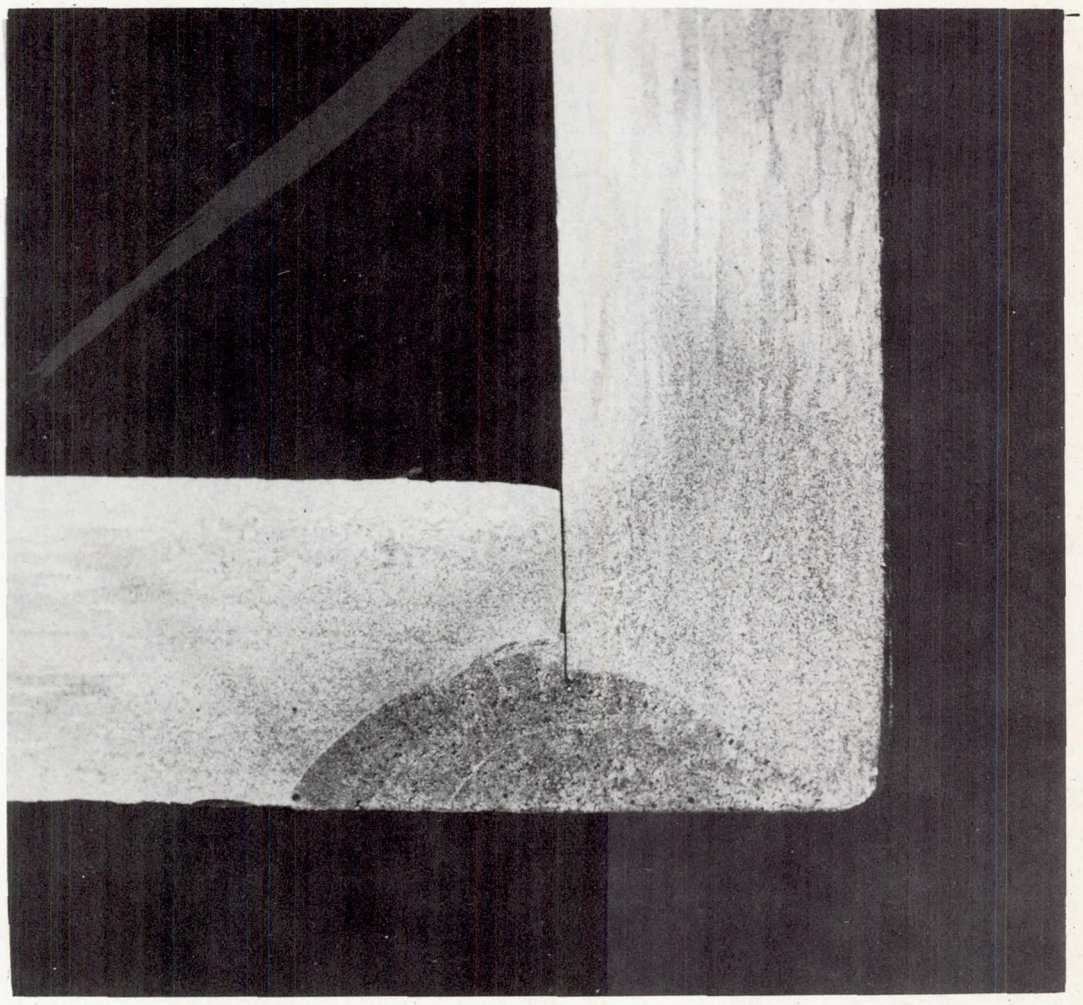

L-87831

Figure 5.- Photomicrograph of a typical section of corner welds. X7.